ARTICLE
Coordinated by Satinder Chopra

Fizz and gas reservoir differentiation based on stochastic inversion

Xin-gang Chi and De-hua Han
Department of Geosciences, University of Houston

AVO attributes of gradient and intercept are related to the reservoir properties based on rock physics knowledge. We develop a new rock physics model based inversion method in this study where we apply the Xu-White shaly-sand mixture model and simultaneously invert the reservoir properties of clay content, water saturation, and porosity with standard deviations from AVO attributes. The method is applied to the seismic data of the Gulf of Mexico at two areas: King Kong and Lisa Anne. After inversion, the fizz and gas reservoirs are differentiated for King Kong and Lisa Anne.

Introduction

Conventionally, the reservoir properties can be inverted first by doing the impedance inversion (P-impedance, S-impedance, or Elastic Impedance inversion) and second by deriving the reservoir properties using the rock physics relationship calibrated from the well. Li et al. (2005) inverted porosity and water saturation from AVO attributes. Chi and Han (2007a and 2007b) inverted reservoir properties from AVO attributes and also developed a method to differentiate fizz and gas reservoirs based on AVO inversion. In this study, we invert reservoir porosity, water saturation, and shale volume with standard deviations directly from seismic AVO attributes.

The rock physics model in this inversion is the Xu-White shaly-sand mixture model (Xu and White, 1995 and 1996; keys and Xu, 2002). The mathematical expressions contained within the shaly-sand mixture model provide a method for determining P-wave velocity, S-wave velocity, and density of the sub-surface rock given shale volume, porosity, and fluid properties as well as properties of minerals and their pore aspect ratios. In this rock physics model, the porosity is incrementally increased by using the differential effective medium theory. After the dry elastic properties are estimated, the bulk modulus and shear modulus of the saturated rock are calculated by using the Gassmann's equation. Then the P-wave velocity, S-wave velocity, and density can be calculated for the saturated rock.

The posterior probability can be written as

$$P(C_j \mid Attributes) = k \times P(Attributes \mid C_j) \times P(C_j),$$

where C_j is the water saturation, porosity, and shale volume, *Attributes* are the intercept and gradient, $P(C_j)$ is the probability density function for C_j, and $P(Attributes \mid C_j)$ is the conditional probability of *Attributes* given C_j. The posterior probability $P(C_j \mid Attributes)$ is calculated as the combination of the prior probability function, the likelihood function, and the normalization coefficient k. When $P(C_j)$ has an uniform distribution, the posterior probability is directly proportional to the likelihood function.

The forward modeling

A two half-space model is constructed to test the effects of porosity, water saturation, and shale volume on intercept and gradient. The top space in the model is shale and the bottom one is sand. Given sand and shale properties in the model, the intercept and gradient can be calculated in different incident angles. The shale properties are the averaged values of well logs in shale segment and the sand properties are calculated in forward modeling based on the shaly-sand mixture model. For the sand, the porosity is from 0.1 to 0.4, the shale volume is from 0 to 0.3, and the water saturation is from 0 to 0.9. In this study, it is assumed that porosity, shale volume and water saturation vary independently.

The parameters used in the modeling shown in the following tables:

	P-velocity (km/s)	S-velocity (km/s)	Density (g/cc)
Shale	2.59	1.10	2.33

Table 1. The parameters of top shale

	Shale	Sand
Pore aspect ratio	0.04	0.15

Table 2. Pore aspect ratios of shale and sand

In the forward modeling, the porosity, water saturation, and shale volume of the sand are varying at the same time. Since the P-wave velocity, S-wave velocity, and density of the sand change with porosity, water saturation, and shale volume in forward modeling, the calculated intercept and gradient are the functions of porosity, water saturation, and shale volume.

Figure 1 shows that results of intercept as function of porosity, water saturation, and shale volume, which are combined randomly in forward modeling. Figure 1a is the projection of intercept on porosity axis, Figure 1b is the projection of intercept on water saturation axis, and Figure 1c is the projection of intercept on shale volume. For instance, if there are no variations of water saturation and shale volume in Figure 1a, there will be a single line to show intercept decreases with increasing porosity. Based on Figure1, the intercept decreases when increasing porosity or shale volume and increases when increasing water saturation.

Figure 2 shows that results of gradient after drawing porosity, water saturation, and shale volume randomly in forward modeling, which is similar to Figure 1. Based on Figure 2, the gradient increases when increasing porosity or shale volume and decreases when increasing water saturation.

Continued on Page 53

Fizz and gas reservoir differentiation based on stochastic inversion

Continued from Page 52

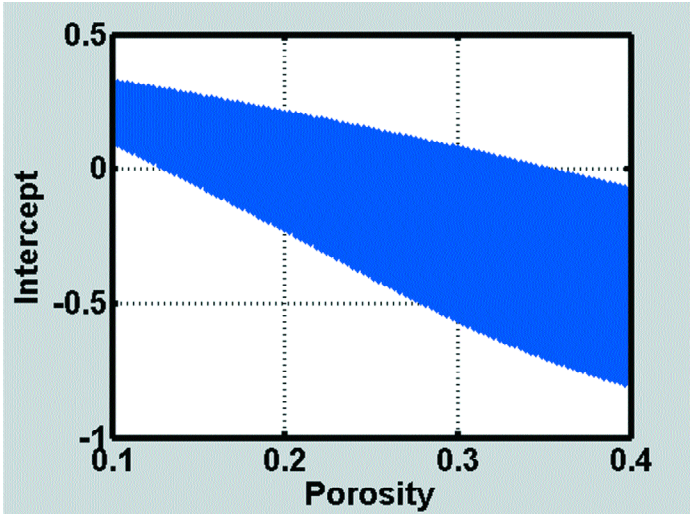

(a) projection of intercept on porosity axis

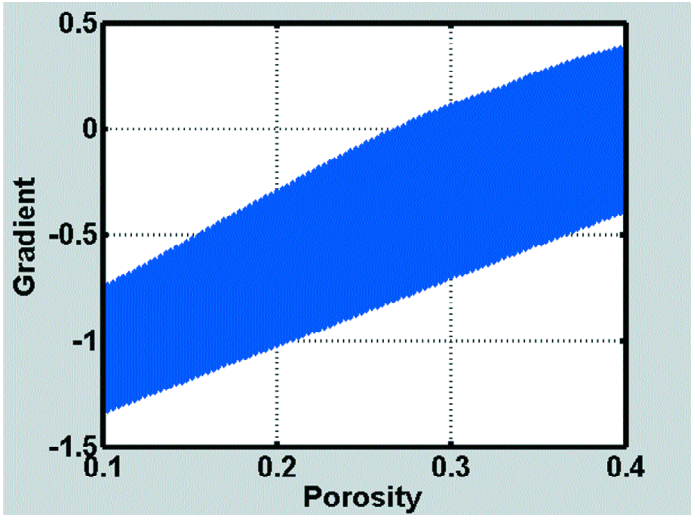

(a) projection of gradient on porosity axis

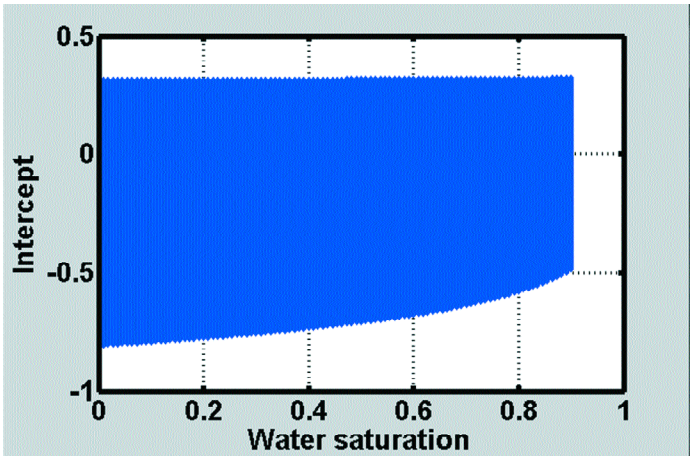

(b) Projection of intercept on water saturation axis

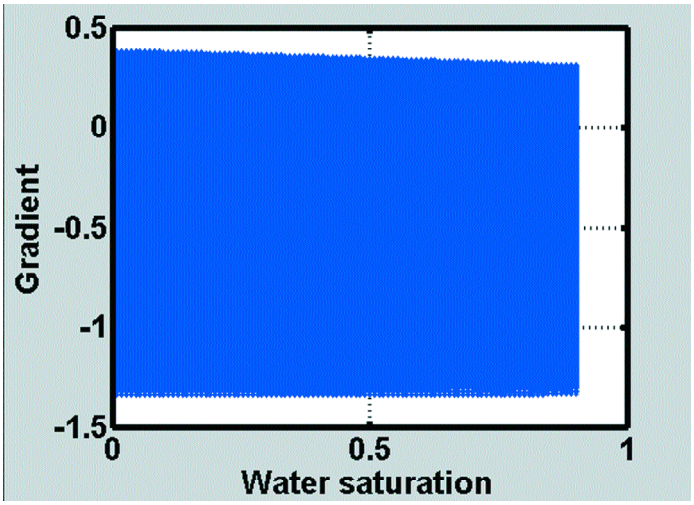

(b) Projection of gradient on water saturation axis

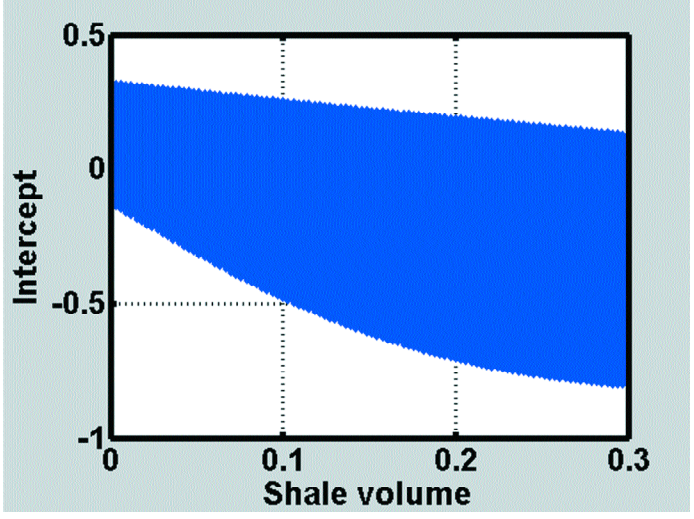

(c) Projection of intercept on shale volume axis

Figure 1. The intercept after stochastic modeling.

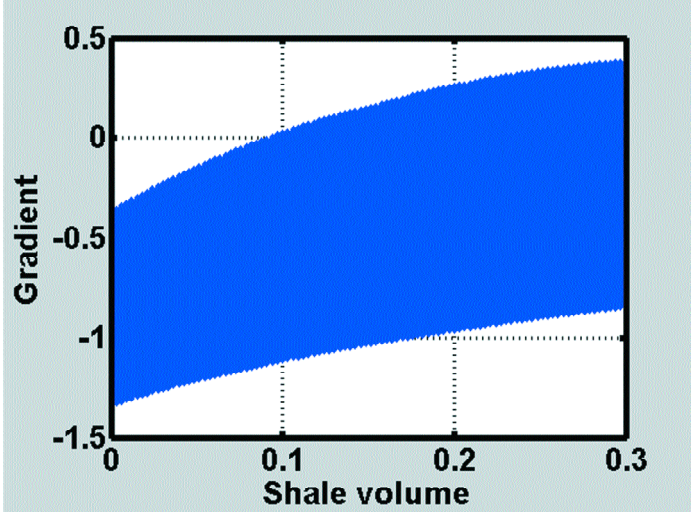

(c) Projection of gradient on shale volume axis

Figure 2. The gradient after stochastic modeling.

Continued on Page 54

Continued from Page 53

The conditional probability

The conditional probability describes the probability for intercept or gradient given certain conditions of porosity, shale volume, and water saturation. In this inversion procedure, the conditional probability is derived from stochastic modeling and combined with the prior probability to calculate the posterior probability for reservoir properties.

Figure 3 shows the probability of intercept given three ranges of porosity, water saturation, or shale volume. The red curve represents the smallest range and the black curve represents the largest range. The blue curve is in the middle range. Figure 3a shows the intercept decreases with increasing porosity and the intercept has

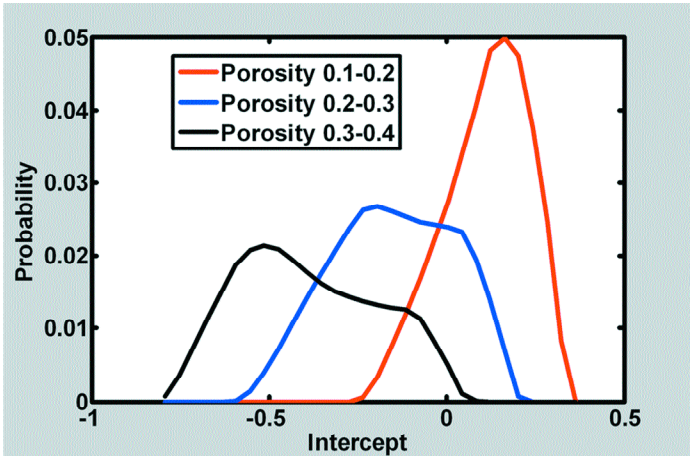

(a) The conditional probability given range of porosity

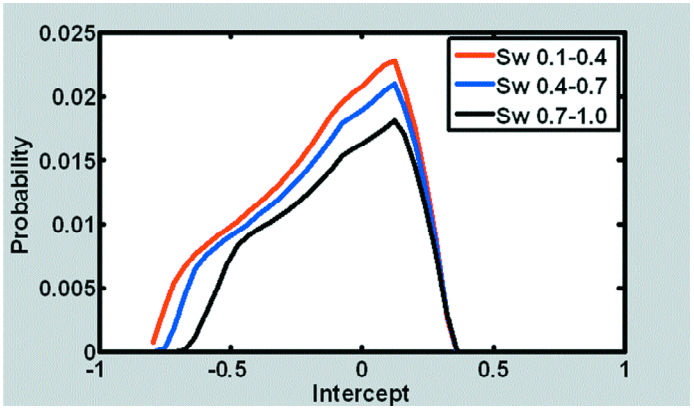

(b) The conditional probability given water saturation

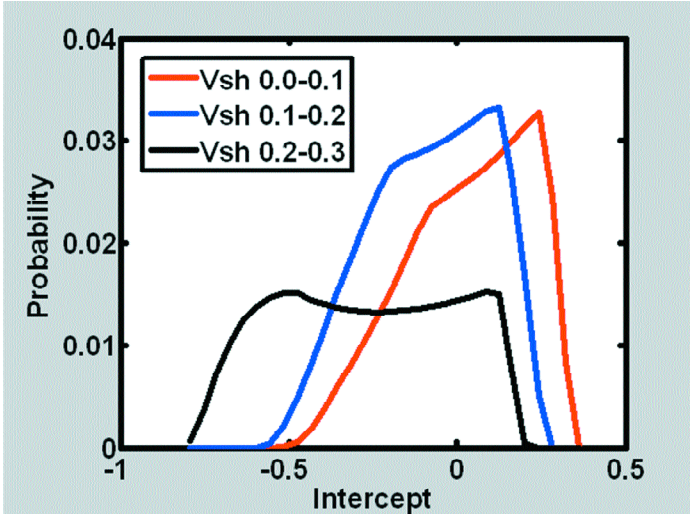

(c) The conditional probability given range of shale volume

Figure 3. The conditional probability of intercept given ranges of porosity, water saturation, and shale volume. (Sw is water saturation and Vsh is shale volume).

Figure 4a shows the probability of gradient given three ranges of porosity. The red curve represents the smallest range and the black curve represents the largest range. The blue curve is in the middle range. The gradient decreases with increasing porosity and the gradient has

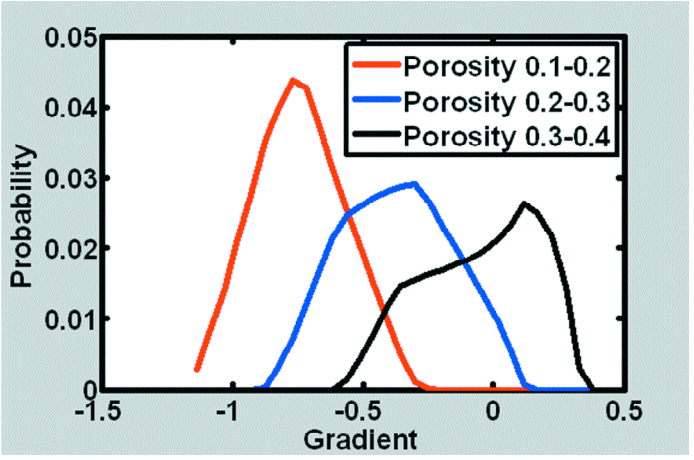

(a) The conditional probability of gradient given range of porosity

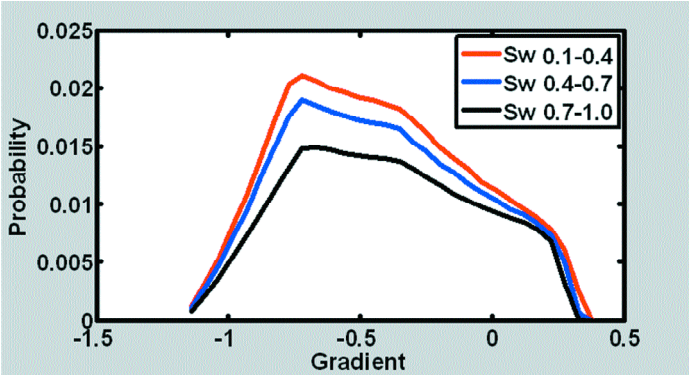

(b) The conditional probability of gradient given range of water saturation

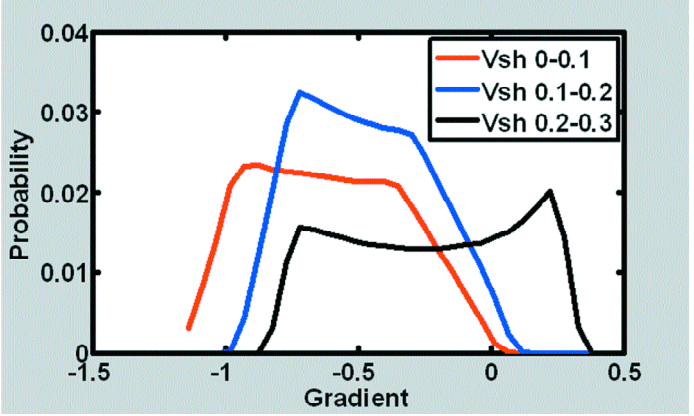

(c) The conditional probability of gradient given range of shale volume

Figure 4. The conditional probability of gradient given ranges of porosity, water saturation, and shale volume. (Sw is water saturation and Vsh is shale volume).

Continued on Page 55

Fizz and gas reservoir differentiation based on stochastic inversion

Continued from Page 54

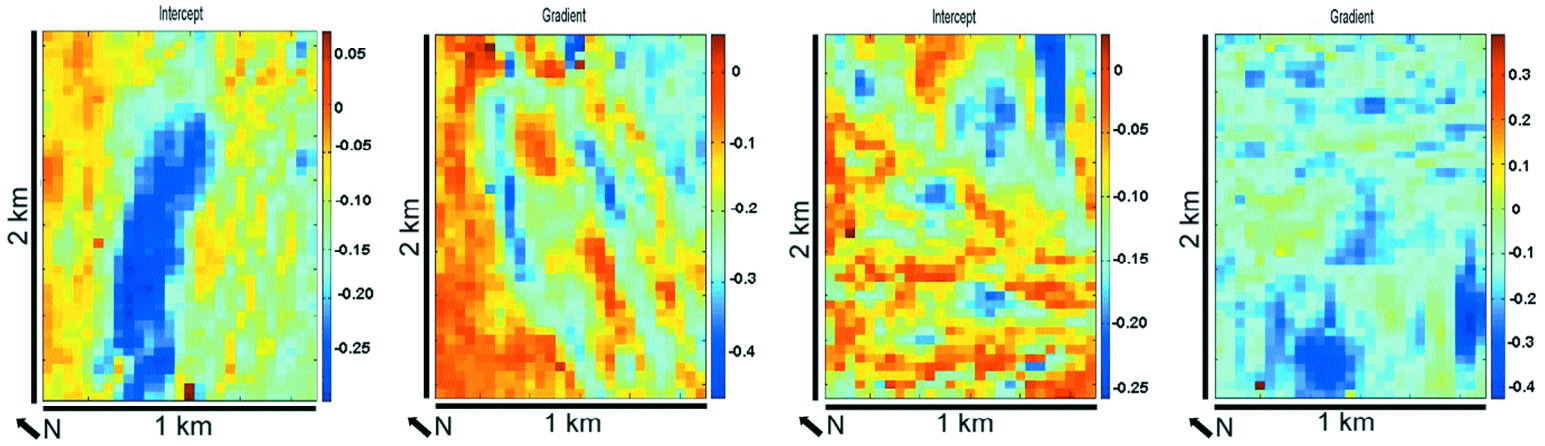

(a) The intercept of King Kong *(b) The gradient of King Kong* *(c) The intercept of Lisa Anne* *(d) The gradient of Lisa Anne*

Figure 5. The intercept and gradient of King Kong and Lisa Anne. The King Kong well logs are used to calibrate the intercept and gradient which are derived from seismic angle gathers.

higher probability in the lower range of porosity. Figures 3b and 3c show that the intercept has the lower probability when water saturation and shale volume are in the higher ranges.

Figure 4 shows the probability of gradient given three ranges of porosity, water saturation, or shale volume, which is similar to Figure 3. Figure 4a shows the gradient increases with increasing porosity and the gradient has higher probability in the lower range of porosity. Figures 4b and 4c show that the gradient has the lower probability when water saturation and shale volume are in the higher ranges.

The case study

In this study, we utilize seismic datasets acquired from King Kong and Lisa Anne in the deepwater Gulf of Mexico. King Kong is located in the western flank of a minibasin controlled by the underlying salt body while Lisa Anne is located in the southeastern flank (O'Brien, 2004). The targets in both of the two fields are unconsolidated sand reservoirs. The top and bottom layers are shale.

In this study, we assume that King Kong is drilled, Lisa Anne is not drilled, and the target reservoirs of King Kong and Lisa Anne have similar thickness. Thus, we can estimate the porosity, water saturation, and shale volume for King Kong after drilling and predict them for Lisa Anne before drilling.

Figure 5 shows the intercept and gradient which are derived from the seismic angle gathers at King Kong and Lisa Anne. The King Kong well logs are used to calibrate the derived intercept and gradient.

After the inversion, the final estimations and standard deviations of porosity, water saturation, and shale volume for King Kong are plotted in Figure 6.

After the inversion, the final predictions and standard deviations of porosity, water saturation, and shale volume for Lisa Anne are plotted in Figure 7.

Continued on Page 56

Fizz and gas reservoir differentiation based on stochastic inversion

Continued from Page 55

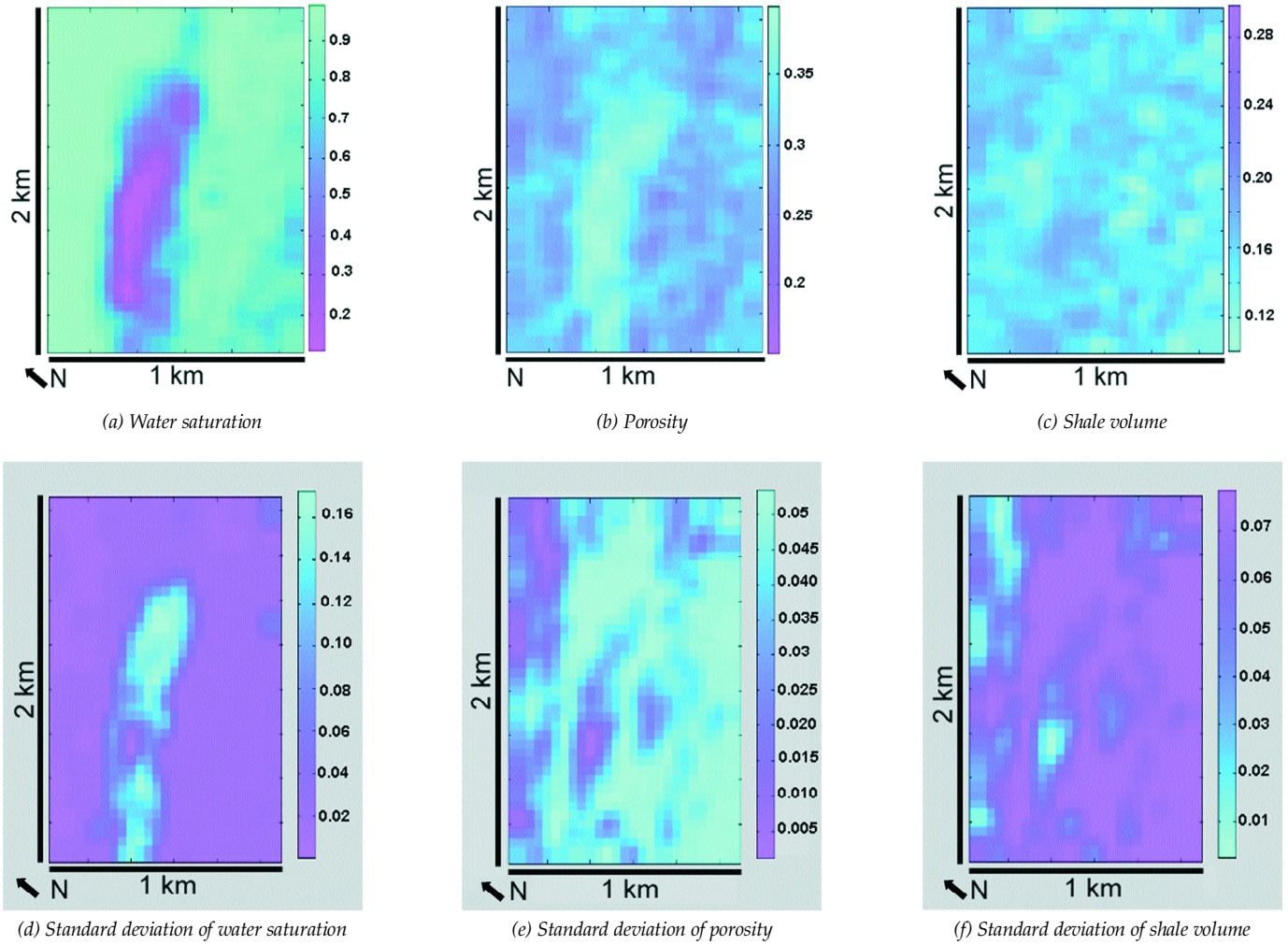

(a) Water saturation *(b) Porosity* *(c) Shale volume*

(d) Standard deviation of water saturation *(e) Standard deviation of porosity* *(f) Standard deviation of shale volume*

Figure 6. The estimated porosity, water saturation, and shale volume with standard deviations at King Kong.

After inversion, the distribution of gas-saturated zone at King Kong is estimated and the fluid property of Lisa Anne is predicted. The inversion results show that King Kong is gas-saturated and Lisa Anne is fizz-saturated. The porosity and shale volume are simultaneously inverted with water saturation for King Kong and Lisa Anne. The inverted results of King Kong and Lisa Anne are consistent with drilling results. The standard deviations show the estimation and prediction confidence for the inversion results. The water saturation has higher standard deviation than the porosity and shale volume.

Conclusions

In this study, the shaly-sand mixture model based inversion method is applied to the seismic data of the Gulf of Mexico. We simultaneously invert water saturation, shale volume, and porosity for the reservoirs of King Kong and Lisa Anne based on the fact that AVO attribute are related to rock properties. The inversion results show the distribution of water saturation, shale volume and porosity for King Kong and the prediction of water saturation, shale volume and porosity for Lisa Anne. The predicted fizz saturation at Lisa Anne is consistent with drilling result. This inversion procedure is a practical way which can be applied to other areas to differentiate fizz and gas reservoir and predict reservoir properties. R

Acknowledgements

We wish to thank sponsors of UH/CSM Fluid/DHI consortium for their supports. We also thank Anadarko Petroleum and WesternGeco for permission to show the seismic data.

References

Chi, X. and D. Han, 2007a, *Fizz and gas reservoir discrimination by AVO inversion*, SEG, 2007 Annual Meeting, 1740-1744

Chi, X. and D. Han, 2007b, *Reservoir properties inversion from AVO attributes*, SEG, 2007 Annual Meeting, 1868-1872

Keys, R. G., and S. Xu, 2002, *An approximation for the Xu-white velocity model:* Geophysics, 67, 1406–1414.

O'Brien, J., 2004, *Interpreter's Corner-Seismic amplitudes from low gas saturation sands*, The Leading Edge, 23, No. 12, 1236-1234

Tarantola, A., 1987, *Inverse problem theory—Methods for data fitting and model parameter estimation:* Elsevier Science Publ. Co.

Li, X., D. Han, and D. McGuire, 2005, *Inversion of Sw and porosity from seismic AVO*, SEG, 2005 Annual Meeting, 1307-131043.

Xu, S. and R. White, 1995, *A new velocity model for claysand mixtures*, Geophysical Prospecting, 43, 91-118.

Xu. S. and R. White, 1996, *A physical model for shearwave velocity prediction*, Geophysical Prospecting, 44, 687-717.

Continued on Page 57

Fizz and gas reservoir differentiation based on stochastic inversion

Continued from Page 56

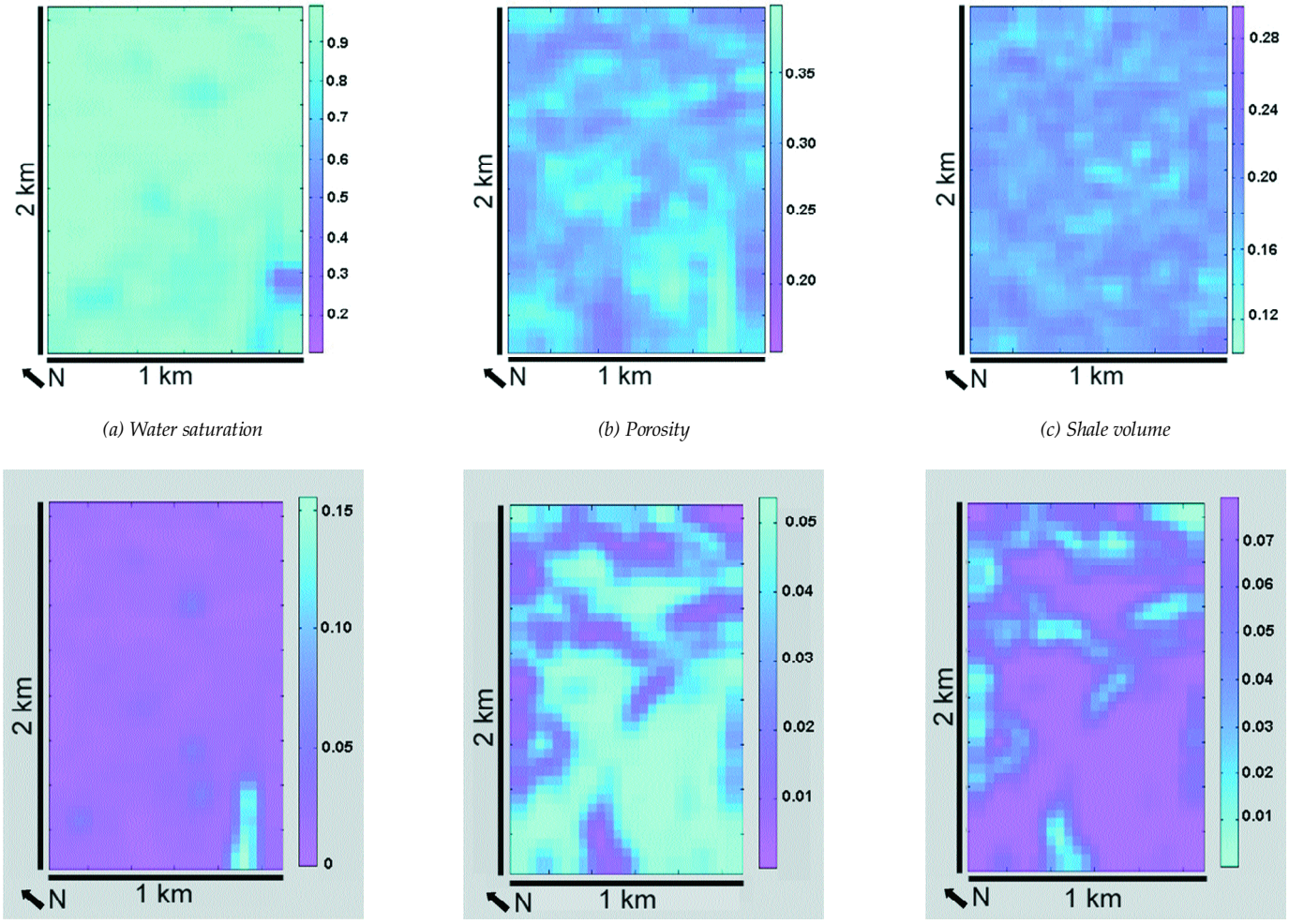

(a) Water saturation

(b) Porosity

(c) Shale volume

(d) Standard deviation of water saturation

(e) Standard deviation of porosity

(f) Standard deviation of shale volume

Figure 7. The predicted porosity, water saturation, and shale volume with standard deviations at Lisa Anne.